

This article was downloaded by: [University Of Gujrat]

On: 11 December 2014, At: 13:56

Publisher: Taylor & Francis

Informa Ltd Registered in England and Wales Registered Number: 1072954 Registered office: Mortimer House, 37-41 Mortimer Street, London W1T 3JH, UK



Molecular Crystals and Liquid Crystals

Publication details, including instructions for authors and subscription information:

<http://www.tandfonline.com/loi/gmcl20>

Properties of ITO/Ga-Al Doped ZnO Bilayer Thin Film for Saving ITO Material

Yu Sup Jung^a, Hyung Wook Choi^a & Kyung Hwan Kim^a

^a Department of Electrical Engineering, Gachon University, Seongnam, Republic of Korea

Published online: 06 Dec 2014.

To cite this article: Yu Sup Jung, Hyung Wook Choi & Kyung Hwan Kim (2014) Properties of ITO/Ga-Al Doped ZnO Bilayer Thin Film for Saving ITO Material, Molecular Crystals and Liquid Crystals, 602:1, 17-25, DOI: [10.1080/15421406.2014.944363](https://doi.org/10.1080/15421406.2014.944363)

To link to this article: <http://dx.doi.org/10.1080/15421406.2014.944363>

PLEASE SCROLL DOWN FOR ARTICLE

Taylor & Francis makes every effort to ensure the accuracy of all the information (the "Content") contained in the publications on our platform. However, Taylor & Francis, our agents, and our licensors make no representations or warranties whatsoever as to the accuracy, completeness, or suitability for any purpose of the Content. Any opinions and views expressed in this publication are the opinions and views of the authors, and are not the views of or endorsed by Taylor & Francis. The accuracy of the Content should not be relied upon and should be independently verified with primary sources of information. Taylor and Francis shall not be liable for any losses, actions, claims, proceedings, demands, costs, expenses, damages, and other liabilities whatsoever or howsoever caused arising directly or indirectly in connection with, in relation to or arising out of the use of the Content.

This article may be used for research, teaching, and private study purposes. Any substantial or systematic reproduction, redistribution, reselling, loan, sub-licensing, systematic supply, or distribution in any form to anyone is expressly forbidden. Terms & Conditions of access and use can be found at <http://www.tandfonline.com/page/terms-and-conditions>

Properties of ITO/Ga-Al Doped ZnO Bilayer Thin Film for Saving ITO Material

YU SUP JUNG, HYUNG WOOK CHOI,
AND KYUNG HWAN KIM*

Department of Electrical Engineering, Gachon University, Seongnam, Republic of Korea

The indium tin oxide (ITO) thin films have advantages such as low resistivity ($\approx 10^{-4} \Omega \cdot \text{cm}$) and high transmittance ($> 85\%$) in visible range. However, Indium in ITO is rare metal, a high cost and toxicity. Therefore, ITO substitute material is necessary. In this study, we fabricated the ITO/Ga-Al doped ZnO (GAZO) bilayer for saving ITO material by using facing targets sputtering methods. The ITO/Ga-Al doped ZnO bilayer thin films were deposited various thicknesses and substrate temperature. As a results, resistivity, mobility and carrier concentration of the ITO(80 nm)/GAZO(100 nm) bilayer thin film at 250°C exhibited $3.79 \times 10^{-4} \Omega \cdot \text{cm}$, $31.13 \text{ cm}^2/\text{V} \cdot \text{s}$ and $5.21 \times 10^{20} \text{ cm}^{-3}$. Average optical transmittances of all ITO/GAZO bilayer thin film exhibited above 90% in visible range.

Keywords: ITO/Ga-Al doped ZnO bilayer; facing targets sputtering; saving ITO material

Introduction

Generally, transparent conductive oxide (TCO) is used many applications such as, liquid crystal display [1], organic light emitting diodes [2], thin film solar cell [3] and smart window [4], etc. One of TCO, the ITO thin film has the lowest resistivity than using TCOs and high transmittance in visible range. However, Indium in ITO is rare metal, a high cost and toxicity. Therefore, ITO substitute material is necessary. The ITO substitute materials, Zinc Oxide (ZnO) [5], Al doped ZnO (AZO) [6], Ga doped ZnO(GZO) [7], Ga-Al doped ZnO(GAZO) [8], tin oxide (SnO_2) [9], and fluorine doped tin oxide (FTO) [10] have been investigated many researchers. One of these materials, The ZnO is n-type semiconductor with the wide direct band gap of 3.37 eV and large exciton binding energy of 60 meV [5]. Furthermore, 3 group material (boron, aluminum, gallium) doped ZnO indicate resistivity below $10^{-3} \text{ ohm} \cdot \text{cm}$ and transmittance above 85% in visible range. Among impurities (B, Al, Ga) doped ZnO materials, low cost, Al doped ZnO material have been widely used. However, Al doped ZnO have disadvantages such as, thermal instability and decreasing conductivity in air. The Ga is less reactive and more resistive to oxidization compared with

*Address correspondence to Prof. K. H. Kim, Department of Electrical Engineering, Gachon University, Bokjeong-dong, Sujeong-gu, Seongnam-si, Gyeonggi-do 461-701, Korea (ROK). E-mail: khkim@gachon.ac.kr

Color versions of one or more of the figures in the article can be found online at www.tandfonline.com/gmcl.

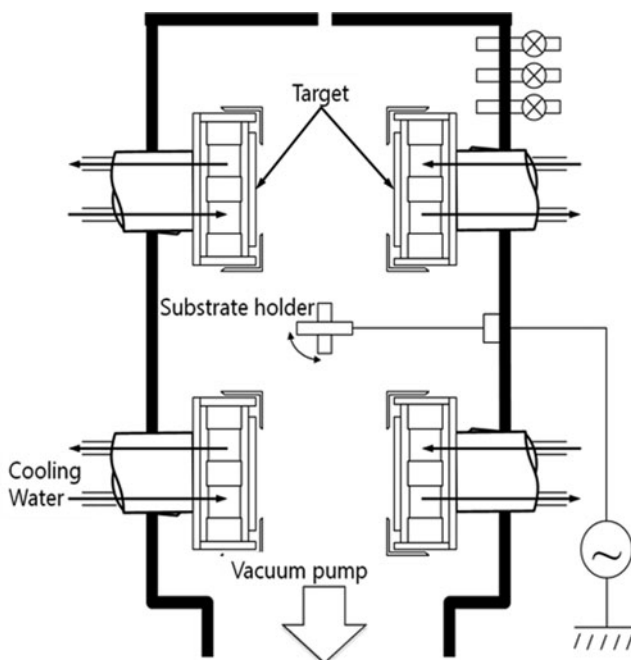


Figure 1. A schematics of facing targets sputtering (FTS) method using the ITO/GAZO bilayer thin film deposition process.

Al. Also, the Ga has ionic and covalent radii of 0.62 and 1.26 Å, respectively, which are closer to the values of Zn (0.74 and 1.31 Å) [11, 12]. The Ga-Al doped ZnO (GZO-AZO) thin films can be deposited by hetero target deposition in facing targets sputtering. In this study, we fabricated the ITO/Ga-Al doped ZnO (GAZO) bilayer thin film for saving ITO material by using facing targets sputtering methods.

Experimental

In this study, we fabricated the ITO/Ga-Al doped ZnO (GAZO) bilayer for saving ITO material by using facing targets sputtering methods. Figure 1 shows schematics of facing targets sputtering method. In Figure 1, In the FTS method, two targets are arranged to face each other. The substrate is located outside of the plasma. Consequently, the FTS method

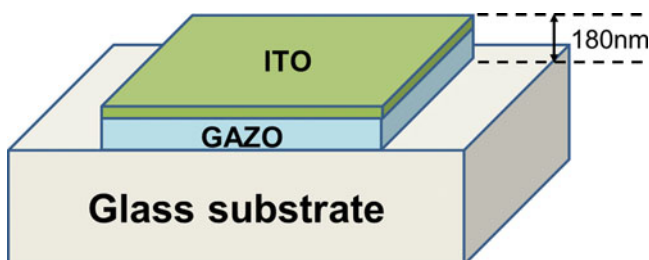


Figure 2. A structure of the ITO/GAZO bilayer thin film.

Table 1. Sputtering condition

Deposition parameter	Sputtering conditions	
Targets	Ga doped ZnO (GZO)	ITO
	Al doped ZnO (AZO)	ITO
Substrate	Glass	
Base pressure	2.6×10^{-4} Pa	
Working pressure	0.4 Pa	
Input power density	1.2 W/cm ²	1.2 W/cm ²
Substrate temperature	Room temperature and 250°C	
Film thickness	GAZO : 100, 120, 140, 160 and 180 nm	ITO : 0, 20, 40, 60, 80 and 180 nm

suppresses the substrate by high-energy particles, such as electrons and ions [13, 14]. Figure 2 shows a structure of the ITO/GAZO bilayer thin film. In this work, the ITO (In₂O₃ : SnO₂ = 90:10 wt.%) targets are installed on top, and the Ga-doped ZnO (ZnO : Ga₂O₃ = 97:3 wt.%) and Al-doped ZnO (ZnO : Al₂O₃ = 98:2 wt.%) targets are installed on the bottom. The sputtering chamber was evacuated to 2.6×10^{-4} Pa (2×10^{-6} Torr) using a rotary pump and turbo molecular pump. The targets were pre-sputtered in argon atmosphere for 30 min in order to remove surface oxidation on the ITO, GZO, and AZO targets. Substrates were ultrasonically cleaned using acetone, ethanol, and deionized water for 10 min, and dried with N₂ gas. Total thicknesses of the ITO/GAZO bilayer were fixed at 180 nm. More details about the sputtering conditions are given in Table 1. The thicknesses of the bilayer thin films were measured using surface profilometry (KLA-Tencor, Alpha-step D-100). The electrical properties of the bilayer thin films were measured using a four-point probe (AIT Co., Ltd, CMT-SR1000N) and Hall measurement (Ecopia, HMS-3000). Optical transmittance was measured using a UV/Vis spectrometer (Hewlett-Packard, 8453). Crystallinity of as-fabricated films was examined by X-ray diffractometer (XRD,

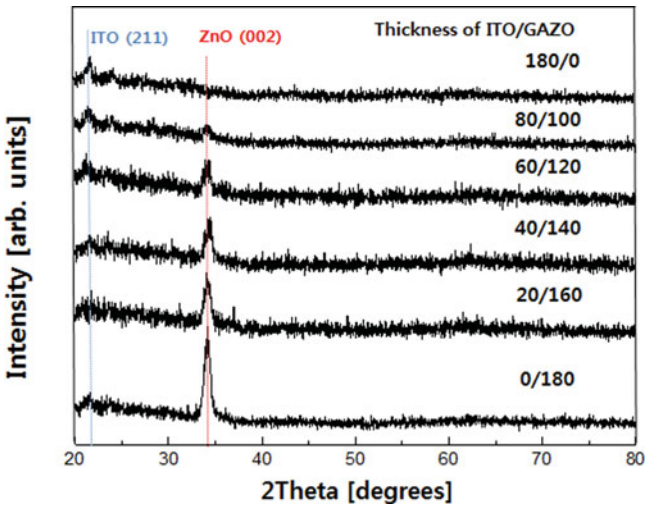


Figure 3. X-ray diffraction peaks of the ITO/GAZO bilayer thin films as a function of thicknesses.

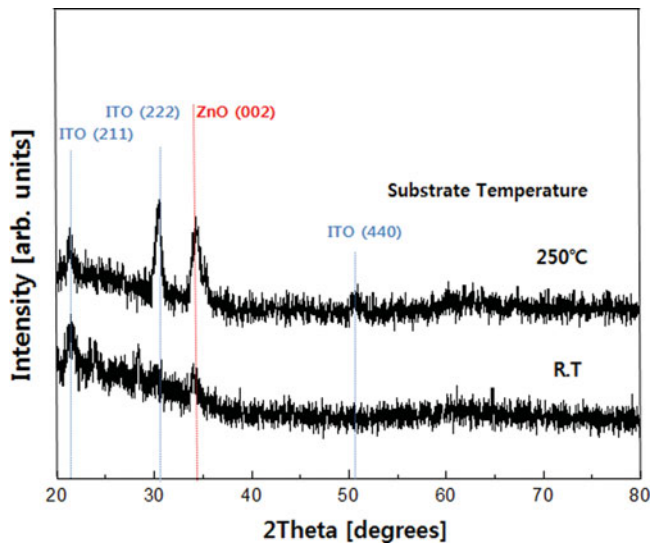


Figure 4. X-ray diffraction peaks of the ITO/GAZO bilayer thin films as a function of substrate temperatures.

D/MAX-2200, Rigaku) with Cu-K α radiation ($\lambda = 1.5418 \text{ \AA}$) X-ray source at 40 kV and 20 mA in the scanning angle (2θ) from 20° to 80° . The surface properties of the bilayer thin film were measured using a field emission scanning electron microscope (FE-SEM, S-4700, Hitachi).

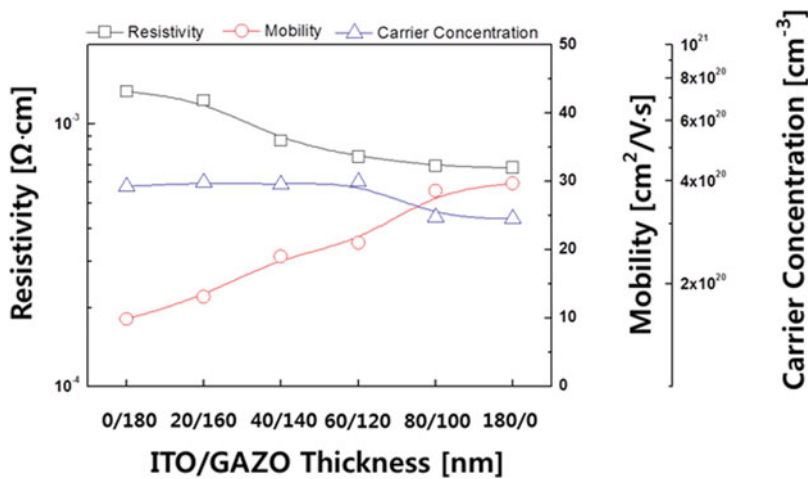


Figure 5. Resistivity, mobility and carrier concentration of the ITO/GAZO bilayer thin films as a function of thicknesses.

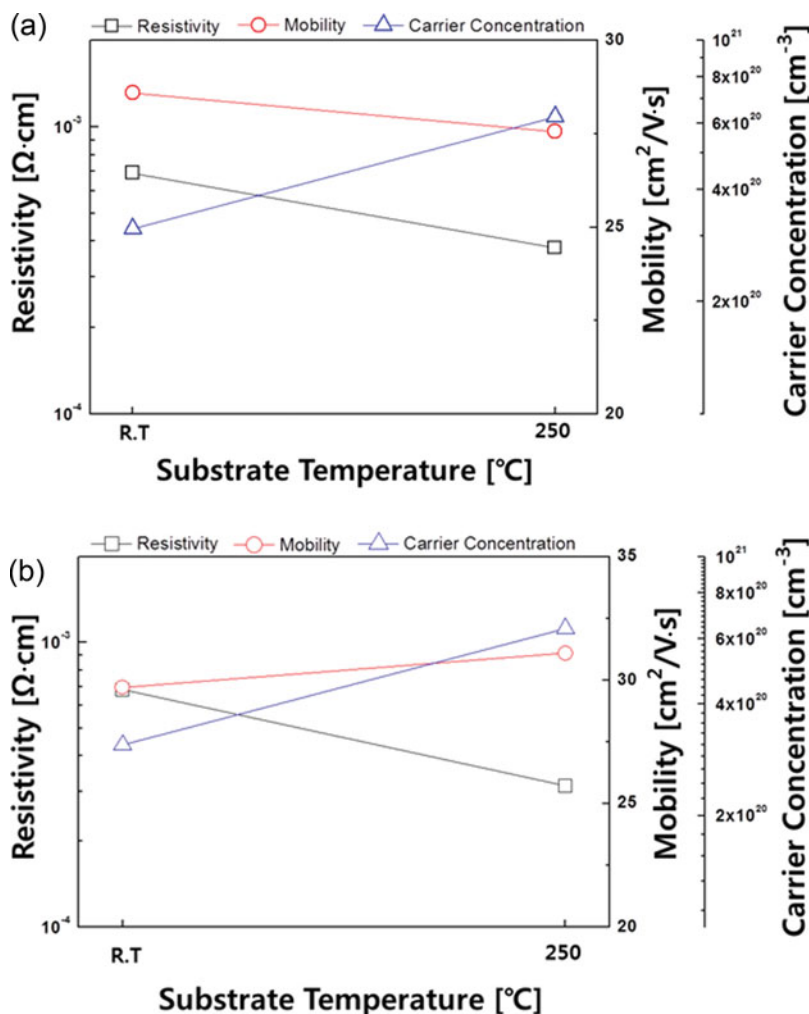


Figure 6. (a) Resistivity, mobility and carrier concentration of the ITO/GAZO bilayer thin films as a function of substrate temperatures. (b) Resistivity, mobility and carrier concentration of the ITO thin film as a function of substrate temperatures.

Results and Discussions

Figure 3 shows that x-ray diffraction peaks of the ITO/GAZO bilayer thin films were deposited as a function of thicknesses at room temperature. In this figure, all the ITO/GAZO bilayer thin films indicated ZnO (002) x-ray diffraction peak at around $2\theta = 34.42^\circ$. Decreasing the thickness of GAZO layer, the ZnO(002) diffraction peak decreased which can be because of low thickness of GAZO thin film layer. When thicknesses of ITO were above 60 nm, the ITO (211) diffraction peak was indicated at around $2\theta = 21.49^\circ$ which can be because of high thickness of ITO thin film layer.

Figure 4 shows that x-ray diffraction patterns of the ITO(80 nm)/GAZO(100 nm) bilayer thin films were deposited at room temperature and 250°C. When the ITO(80 nm)/GAZO(100 nm) bilayer thin film was deposited at room temperature, ZnO (002)

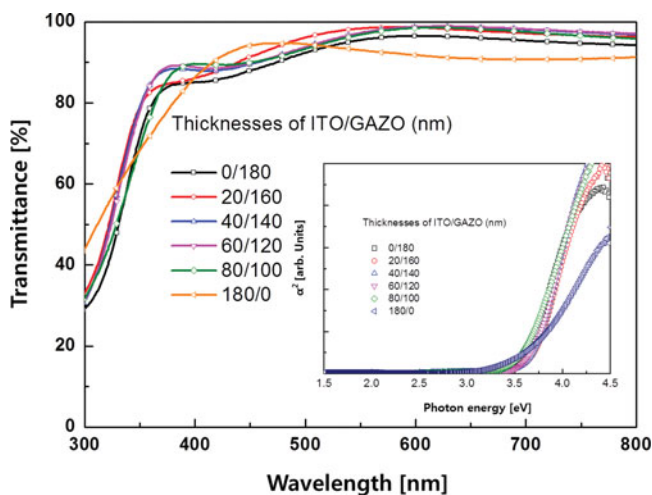


Figure 7. Optical transmittance of the ITO/GAZO bilayer thin films as a function of thicknesses.

and ITO(211) diffraction peaks were indicated slightly. When the ITO/GAZO thin film was deposited at 250°C, ITO(222) and ZnO (002) diffraction peaks were indicated strongly around $2\theta = 30.58^\circ$ which corresponds to the (222) plane of In_2O_3 [15, 16]. As the x-ray diffraction results, the preferred orientation appeared to ITO (222) direction. Also, ITO (440) diffraction peak was indicated slightly around $2\theta = 51.03^\circ$.

Figure 5 shows that resistivity, mobility and carrier concentration of the ITO/GAZO bilayer thin films were deposited as a function of thickness at room temperature. It is seen that thicknesses of ITO layer in ITO/GAZO bilayer increased, resistivity of bilayer decreased. The resistivity of bilayer thin films exhibits a minimum of $6.91 \times 10^{-4} \Omega\cdot\text{cm}$ at 80 nm (ITO thickness) and a maximum of $1.33 \times 10^{-3} \Omega\cdot\text{cm}$ at 0 nm. Increasing thickness of the ITO layer, resistivity of ITO/GAZO bilayer thin film decreased due to the mobility of ITO/GAZO bilayer thin film improved. The mobility was enhanced with improved crystallinity of ITO thin film layer. In addition, the resistivity of ITO (80 nm)/GAZO (100 nm) bilayer thin film was nearly similar to ITO (180 nm) thin film.

Figure 6(a) and (b) show that resistivity, mobility and carrier concentration of the ITO(80 nm)/GAZO (100 nm) bilayer thin film and ITO thin film were deposited at room temperature and 250°C. The resistivity of bilayer thin film exhibits a minimum of $3.79 \times 10^{-4} \Omega\cdot\text{cm}$ at 250°C and a maximum of $6.91 \times 10^{-4} \Omega\cdot\text{cm}$ at room temperature. The resistivity of ITO thin film exhibits a minimum of $3.13 \times 10^{-4} \Omega\cdot\text{cm}$ at 250°C and a maximum of $6.81 \times 10^{-4} \Omega\cdot\text{cm}$ at room temperature. The crystallinity of bilayer thin film improved by increasing substrate temperature, which can be caused increasing the grain size and decreasing the grain boundary. Therefore, the resistivity of thin film decreased with increasing carrier concentration of bilayer.

Figure 7 shows that optical transmittance and optical bandgap energy of ITO/GAZO bilayer thin films and ITO thin film were deposited as a function of thickness at room temperature. As seen in this figure, average optical transmittances in visible range (380–770 nm) of deposited ITO/GAZO bilayer thin film exhibited above 90%. The optical band gap of the ITO/GAZO bilayer thin film and ITO thin film were determined using the Tauc model

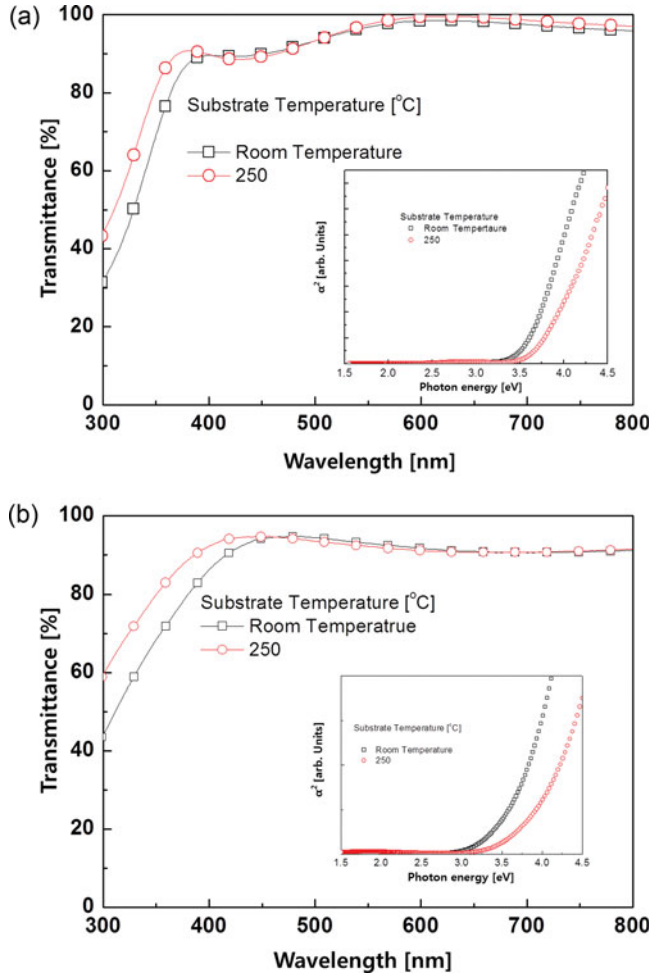


Figure 8. (a) Optical transmittance and optical bandgap of the ITO/GAZO bilayer thin films as a function of substrate temperatures. (b) Optical transmittance and optical bandgap of the ITO thin film as a function of substrate temperatures.

[17] and Davis and Mott model [18] in the high absorbance region

$$(\alpha h\nu) = D(h\nu - E_g)^{1/2} \quad (1)$$

The optical bandgap (E_g) of the thin films can be obtained by plotting α^2 and $h\nu$ (α is the absorption coefficient and $h\nu$ is the photon energy) and extrapolating the linear portion of this plot to the energy axis, as shown figure 7. The absorption edge was shifted to the long wavelength as the ITO thickness increased. The cause of the phenomenon was resulted from the Burstein-Moss effect [19, 20]. According to the B-M effect, the optical band gap can be expressed as:

$$E_g = E_{go} + \Delta E_g = E_{go} + \left(\frac{h}{8m^*} \right) \left(\frac{1}{\pi} \right)^{1/3} n^{2/3} \quad (2)$$

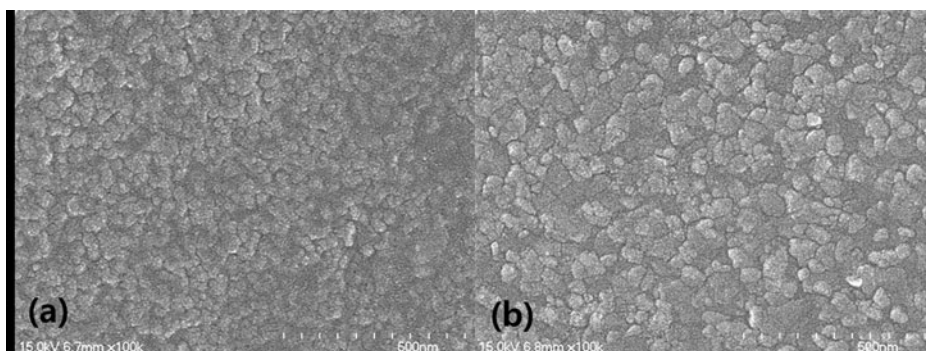


Figure 9. (a)–(b) A surface SEM images of the ITO/GAZO bilayer thin film at room temperature and 250°C.

Where E_{go} is the band gap of undoped ZnO, E_g is the band gap shift caused by B–M effect, n is the carrier concentration. In addition, average optical transmittances of the bilayer thin films were higher than transmittances of ITO and GAZO single layers.

Figure 8(a) and (b) show that optical transmittance of ITO/GAZO bilayer thin film and ITO thin film were deposited at room temperature and 250°C. The absorption edge was shifted to the short wavelength as the substrate temperature increased. The change in the Burstein-Moss shift is due to a change in the carrier concentration with increasing substrate temperature. In this figure, the optical band gap of ITO/GAZO bilayer thin film and ITO thin film were indicated at room temperature and 250°C. The optical bandgap of bilayer thin films exhibited 3.57 eV and 3.7 eV with room temperature and 250°C, The optical bandgap of ITO thin film exhibited 3.45 eV and 3.75 eV with room temperature and 250°C

Figure 9(a) and (b) show that surface SEM images of ITO/GAZO bilayer thin films were deposited at room temperature and 250°C. In this figure, grain size of deposited bilayer thin film at 250°C is greater than deposited bilayer thin film at room temperature. Improved crystallinity of bilayer thin film can be influenced grain size of thin film.

Conclusions

We fabricated the ITO/GAZO bilayer thin films for ITO saving material various thicknesses and substrate temperatures. When the ITO(80 nm)/GAZO(100 nm) bilayer thin films was deposited at 250°C, the strong ITO(222) and ZnO(002) x-ray diffraction peaks and weak ITO(211) and ITO(440) diffraction peaks were indicated which corresponds to the (222)(211)(440) plane of In_2O_3 and (002) plane of ZnO. Resistivity, mobility and carrier concentration of the ITO (80 nm)/GAZO(100 nm) bilayer thin films at 250°C exhibited $3.79 \times 10^{-4} \Omega \cdot cm$, $31.13 cm^2/V \cdot s$ and $5.21 \times 10^{20} cm^{-3}$. Average optical transmittance in visible range (380–770 nm) of all bilayer thin films exhibited above 90% and the optical bandgap of bilayer thin films exhibited 3.7 eV at 250°C. Therefore, the ITO(80 nm)/GAZO(100 nm) bilayer thin films could be applied as transparent conductive electrodes.

Funding

This work was supported by the Human Resources Development Program (No. 20124030200010) of the Korea Institute of Energy Technology Evaluation and Planning (KETEP) grant funded by the Korean government's Ministry of Trade, Industry and Energy.

References

- [1] Yamamoto, N., Makino, H., Osone, S., Ujihara, A., Ito, T., Hokari, H., Maruyama, T., & Yamamoto, T. (2012). *Thin Solid Films*, 520, 4131.
- [2] Tseng, Z. L., Kao, P.C., Yang, C.S., Juang, Y.D., & Chu, S.Y. (2012). *Appl. Surf. Sci.*, 261, 360.
- [3] Lee, D. W., Kwon, O. Y., Song, J. K., Park, C. H., Park, K. E., Nam, S. M., & Kim, Y. N. (2012). *Sol. Energy. Mat. Sol. Cells*, 103, 15.
- [4] Kim, M. H., Kang, T. Y., Jung, Y. S., & Kim, K. H. (2013). *Jpn. J. Appl. Phys.*, 52, 05EC03.
- [5] Iwata, K., Sakemi, T., Yamada, A., Fons, P., Awai, K., Yamamoto, T., Shirakata, S., Matsubara, K., Tampo, H., Sakurai, K., Ishizuka, S., & Niki, S. (2005). *Thin Solid Films*, 480–481, 199.
- [6] Wang, F. H., Chang, H. P., Tseng, C. C., Huang, C. C., & Liu, H. W. (2011). *Curr. Appl. Phys.*, 11, S12.
- [7] Lee, S. H., Cheon, D. K., Kim, W. J., Ham, M. H., & Lee, W. (2012). *Appl. Surf. Sci.*, 258, 6537.
- [8] Hong, J. S., Matsushita, N., & Kim, K. H. (2013). *Thin Solid Films*, 531, 238.
- [9] Seo, Y. J., Kim, G. W., Sung, C. H., Anwar, M. S., Lee, C. G., & Koo, B. H. (2011). *Curr. Appl. Phys.*, 11, S310.
- [10] Kuantama, E., Han, D. W., Sung, Y. M., Song, J. E., & Han, C. H. (2011). *Thin Solid Films*, 519, 4211.
- [11] Kato, H., & Sano, M. (2002). *J. Crystal Growth*, 538, 237.
- [12] Kim, K. H., Choi, H. W., & Kim, K. H. (2013). *J. Nanosci. Nanotechnol.*, 13, 6293.
- [13] Matsushita, N., Ichinose, M., Nakagawa, S., & Naoe, M. (1999). *J. Magn. Magn. Mater.*, 193, 68.
- [14] Jung, Y. S., & Kim, K. H. (2012). *Mat. Res. Bull.*, 47, 2895.
- [15] Liu, C. C., Liang, Y. C., Kuo, C. C., Liou, Y. Y., Chen, J. W., & Lin, C. C. (2009). *Sol. Energy Mater. Sol. Cells*, 93, 267.
- [16] Wang, C., Mao, Y., & Zeng, X. (2013). *Appl. Phys. A*, 110, 41.
- [17] Tauc, J. (1968). *Mat. Res. Bull.*, 3, 37.
- [18] David, A., & Mott, N. F. (1970) *Philos. Mag.*, 22, 903.
- [19] Burstein, E. (1954). *Phys. Rev.*, 93, 632.
- [20] Moss, T. S. (1954). *Proc. Phys. Soc. London, Sect. B*, 67, 775.